RESEARCH ARTICLE | NOVEMBER 19 2024

Detection of antiferromagnetic order in a RuO_2/Pt bilayer by spin Hall magnetoresistance

Yuta Kobayashi ; Shutaro Karube ; Itaru Sugiura ; Hideki Narita ; Ryusuke Hisatomi ; Yoichi Shiota ; Teruo Ono

AIP Advances 14, 115120 (2024)
https://doi.org/10.1063/5.0213320
CHORUS

Detection of antiferromagnetic order in a RuO_2/Pt bilayer by spin Hall magnetoresistance

Cite as: AIP Advances 14, 115120 (2024); doi: 10.1063/5.0213320
Submitted: 16 September 2024 • Accepted: 24 October 2024 •
Published Online: 19 November 2024

Yuta Kobayashi,[1] Shutaro Karube,[1,2,3,a)] Itaru Sugiura,[1] Hideki Narita,[1,3] Ryusuke Hisatomi,[1,2,3] Yoichi Shiota,[1,2] and Teruo Ono[1,2,b)]

AFFILIATIONS

[1] Institute for Chemical Research, Kyoto University, Gokasho, Uji, Kyoto 611-0011, Japan
[2] Center for Spintronics Research Network, Kyoto University, Uji, Kyoto 611-0011, Japan
[3] PRESTO, Japan Science and Technology Agency, Kawaguchi, Saitama 322-0012, Japan

[a)] **Author to whom correspondence should be addressed:** karube.shutaro.8s@kyoto-u.ac.jp
[b)] ono@scl.kyoto-u.ac.jp

ABSTRACT

Altermagnets have spin-split band structures that correspond to the rotational symmetry of the two sublattices in real space. Theoretically, their unique band structures are expected to exhibit intriguing transport phenomena, depending on their magnetic structures. Anomalous Hall effect (AHE) measurement is a method by which to electrically detect magnetic structure and has been reported for typical altermagnets, such as RuO_2 and MnTe. However, AHE measurements are limited to specific cases. Thus, it is important to apply other methods by which to determine functionality based on magnetic structure. In this study, we report the spin Hall magnetoresistance (SMR) in a RuO_2 (1 nm)/Pt (10 nm) system. A negative SMR signal is clearly observed, indicating the spin-flop antiferromagnetic structure of RuO_2. Interestingly, a negative SMR was observed, even at 1 T, which is much smaller than the estimated spin-flop field reported in a previous study. This reflects the thinner film of RuO_2 in our study, suggesting that thickness control is effective in adjusting the magnetic anisotropy of RuO_2. In addition, the temperature-dependent SMR measurement revealed the Néel temperature of 1 nm thick RuO_2 to be 70 ± 9 K. Our results show that SMR measurement can serve as an efficient tool to explore the magnetic features in an altermagnet.

INTRODUCTION

Altermagnets are a new class of collinear antiferromagnets that are characterized by opposite-spin sublattices connected by rotations in real space.[1,2] The real-to-momentum space correspondence results in a spin-split band structure with broken time-reversal symmetry. This unique band structure exhibits intriguing transport phenomena, such as giant tunnel magnetoresistance,[3] giant magnetoresistance,[4] anomalous Hall effect,[5–8] and spin-splitter effect.[9–13]

RuO_2 is a typical altermagnet with large spin-splitting and Néel temperatures above room temperature.[1] In the absence of an external magnetic field, the magnetocrystalline anisotropy in RuO_2 tends to align the Néel vector along the *c* axis in the (001) plane of the tetragonal rutile crystal[14,15] [Fig. 1(a)]. In addition, RuO_2 is electrically conductive, which may originate from the spin density wave instability at the Fermi surface.[14] The conduction electrons of RuO_2 have been experimentally detected to be spin-polarized, owing to the exchange interactions determined by the magnetic structure.[11–13]

The unique transport properties of altermagnets are determined by their magnetic structures. Thus, the detection of their magnetic features is important for the efficient control of their functionality. The anomalous Hall effect (AHE) is one way to electrically detect the magnetic structure of an altermagnet.[6–8] In contrast, the AHE is finite only when the applied currents are asymmetric in the two sublattices and the external magnetic field modulates the Berry curvature perpendicular to the current.[6] Therefore, other electrical methods are required to explore the magnetic structures of altermagnets.

One promising method by which to detect the magnetic structures of an altermagnets is spin Hall magnetoresistance (SMR).[16–18] SMR emerges in a multilayer structure with an interface between the magnetic material and heavy metal, in which strong spin–orbit coupling causes a spin current via the spin Hall effect. The diffusion

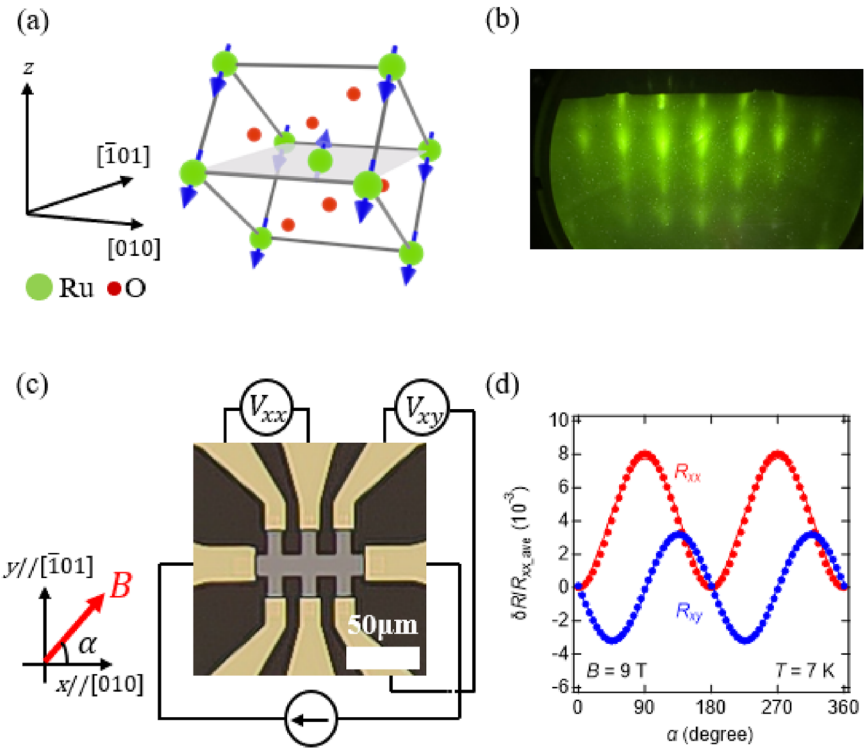

FIG. 1. (a) Crystal and magnetic structure of RuO_2. The crystal plane of (101) is shown in gray. (b) Reflection high-energy electron diffraction (RHEED) images for a RuO_2 (101) surface. (c) Schematic illustration of SMR measurement with the optical micrograph of a fabricated Hall device. (d) Typical SMR signals in the longitudinal δR_{xx} (red) and transverse δR_{xy} (blue) geometries with B = 9 T at 7 K. The solid lines are the fittings with negative SMR functions of $\sin^2\alpha$ and $-\sin 2\alpha$.

of the spin current into the magnetic layer depends on the relative angle of the spin current polarization and magnetic moment, and it results in a change in the magnetoresistance. In cases involving two-sublattice magnets, the expressions for the SMR in the longitudinal and transverse directions are given as[19]

$$\frac{R_{xx}}{R_{xx\_ave}} = \frac{\Delta R}{R_{xx\_ave}} \frac{1}{2}\sum_{i=1}^{2} (1 - {m_{i,y}}^2), \tag{1}$$

$$\frac{R_{xy}}{R_{xx\_ave}} \frac{l}{w} = 2\frac{\Delta R}{R_{xx\_ave}} \frac{1}{2}\sum_{i=1}^{2} (m_{i,x} m_{i,y}), \tag{2}$$

where the x-axis is parallel to the current [Fig. 1(c)], $\frac{l}{w}$ is the geometrical ratio length/width of the Hall bar necessary to compare the longitudinal and transverse resistance, R_{xx_ave} is the resistance irrelevant to the SMR, ΔR represents the SMR coefficient, and $\boldsymbol{m}_i = (m_{i,x}, m_{i,y}, m_{i,z})$ is the unit vector that represents the localized microscopic magnetic moment. When a sufficiently large magnetic field is applied to a collinear antiferromagnet, it takes a spin-flop magnetic configuration in which the Néel vector $\boldsymbol{N} = \frac{\boldsymbol{m}_1 - \boldsymbol{m}_2}{2}$ is orthogonal to the external magnetic field, where $\boldsymbol{m}_{1,2}$ is the magnetic moment of each sublattice. In the measurement setup shown in Fig. 1(c), assuming a spin-flop state for the antiferromagnet, we can rewrite Eqs. (1) and (2) as follows:

$$\frac{R_{xx}}{R_{xx\_ave}} = \frac{\Delta R}{R_{xx\_ave}} \sin^2\alpha, \tag{3}$$

$$\frac{R_{xy}}{R_{xx\_ave}} \frac{l}{w} = -\frac{\Delta R}{R_{xx\_ave}} \sin 2\alpha, \tag{4}$$

where α is the angle of the in-plane magnetic field. Here, we neglect the net magnetization $\boldsymbol{M} = \frac{\boldsymbol{m}_1 + \boldsymbol{m}_2}{2}$, which is usually negligible in collinear antiferromagnets, by canting.[19–24] The angular dependences expressed in Eqs. (3) and (4) are called negative SMR because their signs are reversed with ferromagnetic materials in which the magnetic moment is parallel to the magnetic field.[20,21] Therefore, the SMR measurement can detect the Néel vector projection onto the magnetic field rotation plane.[25–28] It should be noted that in this study, the SMR signals are related not to the absence of time-reversal symmetry in the altermagnets but to the detection of the antiferromagnetic spin structure.

In this study, we explored the magnetic order in a RuO_2 1 nm/Pt 10 nm bilayer using SMR. Negative SMR was observed at a magnetic field above 1 T, indicating a spin-flop magnetic configuration in RuO_2. In addition, the Néel temperature of 1 nm thick RuO_2 was estimated from the temperature dependence of SMR. Our results show that SMR measurements can serve as an efficient tool to explore the magnetic features of an altermagnet.

METHOD

A bilayer film of RuO_2 (1 nm)/Pt (10 nm) was prepared via magnetron sputtering on an Al_2O_3 (1$\bar{1}$02) single-crystalline substrate. During the deposition of RuO_2, the substrate was heated at

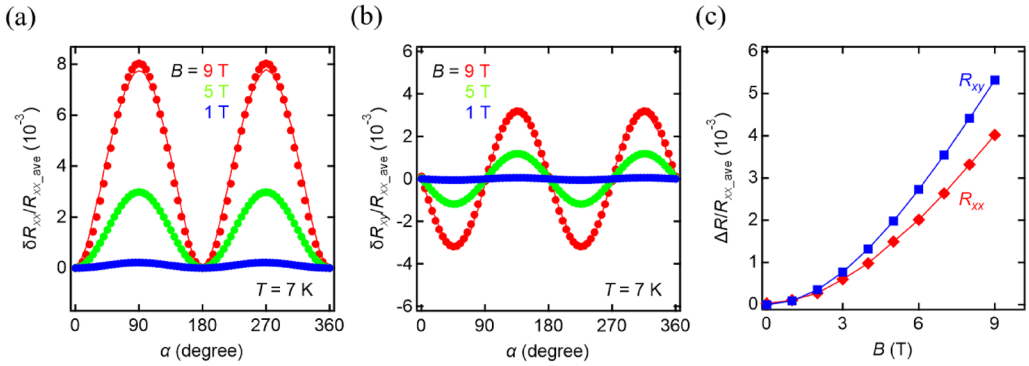

FIG. 2. SMR signals in the (a) longitudinal and (b) transverse geometries, obtained at 7 K with different external magnetic fields. The solid lines are the fittings with negative SMR functions of $\sin^2\alpha$ and $-\sin 2\alpha$. (c) The amplitude of the SMR signal in the longitudinal (red) and transverse (blue) geometries as a function of the external magnetic field at 7 K. Solid lines connect two adjacent points.

400 °C under an Ar pressure of 0.24 Pa with a partial O_2 pressure of 0.06 Pa.

The reflection high-energy electron diffraction (RHEED) patterns of the RuO_2 surface exhibited two-fold symmetry under the in-plane rotation of the sample, indicating the epitaxial growth of the RuO_2 (101) film on the Al_2O_3 ($1\bar{1}02$) substrate. The modulated RHEED image showed that our RuO_2 (101) film has a multilevel stepped surface, as shown in Fig. 1(b).

The bilayer film was photolithographically patterned for transport measurements into a Hall-cross structure with Ar ion milling, and the width of the Hall bar device was 15 μm [Fig. 1(c)].

Electrical transport measurements were performed using a Physical Property Measurement System (PPMS-9T, Quantum Design). In the angle α-dependent measurement described in Fig. 1(c), while rotating the sample under the static field B, the longitudinal resistance R_{xx} and transverse resistance R_{xy} were measured with an electric current of ±1 mA ($J \approx 9.1 \times 10^{10}$ A/m^2) via a current reversal method. Constant offsets were subtracted from R_{xx} and R_{xy} as $\delta R_{xx} = R_{xx} - \min(R_{xx})$ and $\delta R_{xy} = R_{xy} - R_{xy\_ave}$, where $\min(R_{xx})$ is the minimum value of R_{xx} and R_{xy_ave} is the angle-averaged R_{xy}. All results in this study were normalized by the angle-averaged longitudinal resistance R_{xx_ave}. To suppress the drift owing to temperature instability, the measurements at each temperature were performed 3 h after reaching the set value of the temperature. The current shunting ratio of RuO_2 was estimated to be lower than 10^{-5} below 300 K by measuring the resistivity of the RuO_2 1 nm film and Pt 10 nm film deposited on the Al_2O_3 ($1\bar{1}02$) substrate (see the supplementary material for details).

RESULT AND DISCUSSION

Figure 1(d) shows typical SMR signals in the longitudinal (red) and traverse (blue) geometries with B = 9 T at a measurement temperature T of 7 K. Each signal was well-fitted by Eqs. (3) and (4), respectively. These negative SMR signals clearly indicate the spin-flop antiferromagnetic structure of RuO_2. This spin-flop field, which was smaller than 9 T, surprisingly differs from the results of a previous study that showed that the spin-flop field is larger than

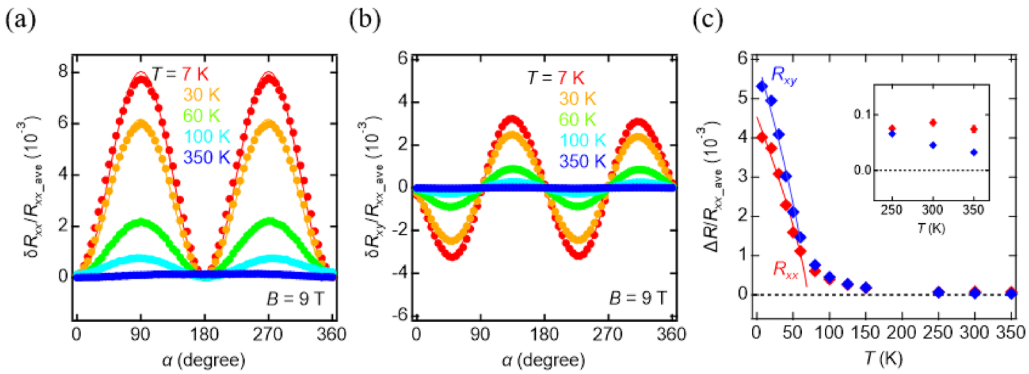

FIG. 3. SMR signals in the (a) longitudinal and (b) transverse geometries with an external magnetic field of 9 T at different temperatures. The solid lines are the fittings with negative SMR functions of $\sin^2\alpha$ and $-\sin 2\alpha$. (c) The amplitude of the SMR signal in the longitudinal (red) and transverse (blue) geometries as a function of temperature with an external magnetic field of 9 T. The solid lines are the fittings with the power law proportional to $(T_N - T)^\nu$ in the range of 7 K ≤ T ≤ 60 K. The inset shows the data for 250 K ≤ T with an enlarged vertical axis.

50 T.[6] This discrepancy could reflect differences in the exchange or anisotropic magnetic fields owing to different film thicknesses.[29–31] Thus, our results suggest that the magnetic structure of RuO_2 can be controlled relatively easily by decreasing the film thickness, which is an important milestone in the study of altermagnets. According to Eqs. (3) and (4), $\frac{\Delta R_{xx}}{R_{xx\_ave}}$ and $\frac{\Delta R_{xy}}{R_{xx\_ave}}\frac{l}{w}$ should be the same amplitude. Each value determined by the fitting was $\frac{\Delta R_{xx}}{R_{xx\_ave}} = (4.02 \pm 0.03) \times 10^{-3}$ and $\frac{\Delta R_{xy}}{R_{xx\_ave}}\frac{l}{w} = (5.32 \pm 0.05) \times 10^{-3}$. The ratio is 0.76. This discrepancy with theory can be attributed to local variations in the spin-mixing conductance.[20] The geometrical ratio factor l/w = 1.67 for our device.

Figures 2(a) and 2(b) show the SMR signal in the longitudinal and transverse geometries with different magnetic fields at 7 K. Figure 2(c) shows the amplitude of the negative SMR determined via fitting with respect to the magnetic field. The amplitude of the negative SMR monotonically increases with the external magnetic field, suggesting that RuO_2 has a multidomain magnetic structure and that the spin-flop phase is driven by the redistribution of the magnetic domain[22] in the magnetic field range of up to at least 9 T. In addition, a negative SMR was observed, even at 1 T, which was the minimum field in our measurement, indicating that the spin-flop field was greatly suppressed by the thickness control.

Figures 3(a) and 3(b) show the SMR signal in the longitudinal and transverse geometries at different temperatures at 9 T. Figure 3(c) shows the amplitude of the negative SMR determined via fitting at various temperatures. Here, $\frac{\Delta R}{R_{xx\_ave}}$ decreases significantly with temperature between 7 and 60 K, has an inflection point near 60 K, and continues to decrease up to 350 K while maintaining the sign of a negative SMR. One possible explanation for this residual negative SMR at temperatures above 60 K is the grain distribution at different Néel temperatures. To estimate the Néel temperature T_N of a majority of the domains, we fitted $\frac{\Delta R}{R_{xx\_ave}}$ in the range of 7 K $\leq T \leq$ 60 K by a power law proportional to $(T_N - T)^{\nu}$, where T_N and the critical exponent ν are the adjustment parameters.[19,26] The obtained values of T_N and ν were 70 ± 9 K and 0.75 ± 0.2 for $\frac{\Delta R_{xx}}{R_{xx\_ave}}$ and 70 ± 9 K and 0.75 ± 0.3 for $\frac{\Delta R_{xy}}{R_{xx\_ave}}\frac{l}{w}$, respectively. The estimated value of T_N was lower than those reported in previous studies, which reported T_N higher than room temperature. This discrepancy can be attributed to different film thicknesses. This decrease in T_N with decreasing film thickness has also been reported for other antiferromagnets.[29–31] In addition, this decrease in T_N was consistent with a relatively small exchange field, as expected from the small spin-flop field. The inhomogeneity of the sample is another possible explanation for the change in SMR amplitude with respect to temperature. However, this is unlikely because the transmission electron microscopy (TEM) image indicated that the RuO_2 film was clean (see the supplementary material for details).

CONCLUSION

In summary, the SMR of a RuO_2/Pt bilayer was studied. A negative SMR was observed over the full temperature range of the measurement, which clearly indicates a spin-flop antiferromagnetic structure in RuO_2. The Néel temperature T_N was estimated to be 70 ± 9 K from the temperature dependence of the SMR. The relatively lower T_N and spin-flop field are considered to be because of the thinner film, compared with that reported in a previous study.[6] Our results show that SMR can be an effective tool to explore magnetic features in an altermagnet, and they suggest that thickness control can be an effective method by which to adjust the magnetic anisotropy of RuO_2.

SUPPLEMENTARY MATERIAL

See the supplementary material for the temperature-dependent resistivity in RuO_2 and Pt and transmission electron microscopy images of RuO_2.

ACKNOWLEDGMENTS

This work was supported by the JSPS KAKENHI (Grant Nos. JP22J12061 and JP20H05665), the JST PRESTO (Grant No. JPMJPR22B4), the Iketani Science and Technology Foundation (Grant No. 0351046-A), the Mazda Foundation, and the Collaborative Research Program of the Institute for Chemical Research, Kyoto University.

AUTHOR DECLARATIONS

Conflict of Interest

The authors have no conflicts to disclose.

Author Contributions

Yuta Kobayashi: Conceptualization (equal); Data curation (equal); Formal analysis (equal); Funding acquisition (equal); Investigation (equal); Methodology (equal); Validation (equal); Visualization (equal); Writing – original draft (equal); Writing – review & editing (equal). **Shutaro Karube**: Conceptualization (equal); Data curation (equal); Funding acquisition (equal); Investigation (equal); Methodology (equal); Resources (equal); Supervision (equal); Validation (equal); Visualization (equal); Writing – original draft (equal); Writing – review & editing (equal). **Itaru Sugiura**: Data curation (equal); Investigation (equal); Methodology (equal); Visualization (equal). **Hideki Narita**: Writing – review & editing (equal). **Ryusuke Hisatomi**: Writing – review & editing (equal). **Yoichi Shiota**: Writing – review & editing (equal). **Teruo Ono**: Conceptualization (equal); Funding acquisition (equal); Resources (equal); Supervision (equal); Validation (equal); Writing – review & editing (equal).

DATA AVAILABILITY

The data supporting the findings of this study are available from the corresponding author upon reasonable request.

REFERENCES

[1] L. Šmejkal, J. Sinova, and T. Jungwirth, Phys. Rev. X **12**, 040501 (2022).
[2] L. Šmejkal, J. Sinova, and T. Jungwirth, Phys. Rev. X **12**, 031042 (2022).
[3] D. F. Shao, S. H. Zhang, M. Li, C. B. Eom, and E. Y. Tsymbal, Nat. Commun. **12**, 7061 (2021).

[4]L. Šmejkal, A. B. Hellenes, R. G. Hernández, J. Sinova, and T. Jungwirth, Phys. Rev. X **12**, 011028 (2022).
[5]L. Šmejkal, R. González-Hernández, T. Jungwirth, and J. Sinova, Sci. Adv. **6**, eaaz8809 (2020).
[6]Z. Feng, X. Zhou, L. Šmejkal, L. Wu, Z. Zhu, H. Guo, R. González-Hernández, X. Wang, H. Yan, P. Qin, X. Zhang, H. Wu, H. Chen, Z. Meng, L. Liu, Z. Xia, J. Sinova, T. Jungwirth, and Z. Liu, Nat. Electron. **5**, 735–743 (2022).
[7]R. Gonzalez Betancourt, J. Zubáč, R. Gonzalez-Hernandez, K. Geishendorf, Z. Šobáň, G. Springholz, K. Olejník, L. Šmejkal, J. Sinova, T. Jungwirth, S. T. B. Goennenwein, A. Thomas, H. Reichlová, J. Železný, and D. Kriegner, Phys. Rev. Lett. **130**, 036702 (2023).
[8]T. Tschirner, P. Keßler, R. D. Gonzalez Betancourt, T. Kotte, D. Kriegner, B. Büchner, J. Dufouleur, M. Kamp, V. Jovic, L. Smejkal, J. Sinova, R. Claessen, T. Jungwirth, S. Moser, H. Reichlova, and L. Veyrat, APL Mater. **11**, 101103 (2023).
[9]L. D. Yuan, Z. Wang, J. W. Luo, E. I. Rashba, and A. Zunger, Phys. Rev. B **102**, 014422 (2020).
[10]R. González-Hernández, L. Šmejkal, K. Výborný, Y. Yahagi, J. Sinova, T. Jungwirth, and J. Železný, Phys. Rev. Lett. **126**, 127701 (2021).
[11]A. Bose, N. J. Schreiber, R. Jain, D. F. Shao, H. P. Nair, J. Sun, X. S. Zhang, D. A. Muller, E. Y. Tsymbal, D. G. Schlom, and D. C. Ralph, Nat. Electron. **5**, 267–274 (2022).
[12]H. Bai, L. Han, X. Y. Feng, Y. J. Zhou, R. X. Su, Q. Wang, L. Y. Liao, W. X. Zhu, X. Z. Chen, F. Pan, X. L. Fan, and C. Song, Phys. Rev. Lett. **128**, 197202 (2022).
[13]S. Karube, T. Tanaka, D. Sugawara, N. Kadoguchi, M. Kohda, and J. Nitta, Phys. Rev. Lett. **129**, 137201 (2022).
[14]T. Berlijn, P. C. Snijders, O. Delaire, H.-D. Zhou, T. A. Maier, H. B. Cao, S. X. Chi, M. Matsuda, Y. Wang, M. R. Koehler, P. R. C. Kent, and H. H. Weitering, Phys. Rev. Lett. **118**, 077201 (2017).
[15]Z. H. Zhu, J. Strempfer, R. R. Rao, C. A. Occhialini, J. Pelliciari, Y. Choi, T. Kawaguchi, H. You, J. F. Mitchell, Y. Shao-Horn, and R. Comin, Phys. Rev. Lett. **122**, 017202 (2019).
[16]Y. T. Chen, S. Takahashi, H. Nakayama, M. Althammer, S. T. B. Goennenwein, E. Saitoh, and G. E. W. Bauer, Phys. Rev. B **87**, 144411 (2013).
[17]N. Vlietstra, J. Shan, V. Castel, J. Ben Youssef, G. E. W. Bauer, and B. J. van Wees, Appl. Phys. Lett. **103**, 032401 (2013).
[18]H. Nakayama, M. Althammer, Y. T. Chen, K. Uchida, Y. Kajiwara, D. Kikuchi, T. Ohtani, S. Geprägs, M. Opel, S. Takahashi, R. Gross, G. E. W. Bauer, S. T. B. Goennenwein, and E. Saitoh, Phys. Rev. Lett. **110**, 206601 (2013).
[19]K. Sugi, T. Ishikawa, M. Kimata, Y. Shiota, T. Ono, T. Kato, and T. Moriyama, Phys. Rev. B **108**, 064434 (2023).
[20]G. R. Hoogeboom, A. Aqeel, T. Kuschel, T. T. M. Palstra, and B. J. van Wees, Appl. Phys. Lett. **111**, 052409 (2017).
[21]Y. Ji, J. Miao, Y. M. Zhu, K. K. Meng, X. G. Xu, J. K. Chen, Y. Wu, and Y. Jiang, Appl. Phys. Lett. **112**, 232404 (2018).
[22]J. Fischer, O. Gomonay, R. Schlitz, K. Ganzhorn, N. Vlietstra, M. Althammer, H. Huebl, M. Opel, R. Gross, S. T. B. Goennenwein, and S. Geprägs, Phys. Rev. B **97**, 014417 (2018).
[23]L. Baldrati, A. Ross, T. Niizeki, C. Schneider, R. Ramos, J. Cramer, O. Gomonay, M. Filianina, T. Savchenko, D. Heinze, A. Kleibert, E. Saitoh, J. Sinova, and M. Kläui, Phys. Rev. B **98**, 024422 (2018).
[24]M. Kimata, T. Moriyama, K. Oda, and T. Ono, Appl. Phys. Lett. **116**, 192402 (2020).
[25]R. Schlitz, T. Kosub, A. Thomas, S. Fabretti, K. Nielsch, D. Makarov, and S. T. B. Goennenwein, Appl. Phys. Lett. **112**, 132401 (2018).
[26]K. Oda, T. Moriyama, M. Kimata, S. Kasukawa, and T. Ono, Jpn. J. Appl. Phys. **59**, 010908 (2020).
[27]J. Xu, M. Jia, C. Zhou, Q. Li, P. Shafer, G. Chen, M. Yang, A. T. N'Diaye, E. Arenholz, Z. Qiu, and Y. Wu, Phys. Rev. B **106**, 134425 (2022).
[28]K. Oda, T. Moriyama, and T. Ono, J. Magn. Soc. Jpn. **43**, 1 (2019).
[29]D. Alders, L. H. Tjeng, F. C. Voogt, T. Hibma, G. A. Sawatzky, C. T. Chen, J. Vogel, M. Sacchi, and S. Iacobucci, Phys. Rev. B **57**, 11623 (1998).
[30]T. Ambrose and C. L. Chien, J. Appl. Phys. **83**, 6822–6824 (1998).
[31]M. S. Lund, W. A. A. Macedo, K. Liu, J. Nogués, I. K. Schuller, and C. Leighton, Phys. Rev. B **66**, 054422 (2002).